Opto-acoustic phenomena in whispering gallery mode resonators

Guoping Lin & Yanne K. Chembo

Taylor & Francis
Taylor & Francis Group

Opto-acoustic phenomena in whispering gallery mode resonators

Guoping Lin and Yanne K. Chembo

Optics Department, FEMTO-ST Institute, Besançon, France

ABSTRACT

Optical whispering gallery mode resonators are important platforms to enhance and study various nonlinear frequency conversion processes. Stimulated Brillouin scattering is one of the strongest nonlinear effects, and can be successfully investigated using these platforms. In this article, we study the phenomenon of stimulated Brillouin scattering using a crystalline disk resonator. A fast scanning ringdown spectroscopy technique is used to characterize the optical modes featuring quality factors of the order of one billion at telecom wavelengths. The mW scale threshold power in a centimeter disk resonator is observed and found to be strongly dependent on the gap between the resonator and the prism coupler.

1. Introduction

Stimulated Brillouin Scattering (SBS) has been the focus of strong interest in the past decades. It is an inelastic scattering that results from the interaction between light and acoustic waves. The acoustic wave can be produced by an intense pump laser through electrostriction. Above a threshold power, the reflected Doppler down-shift Stokes signal becomes significant and in turn strengthens the density wave. The experimental observation of SBS was first observed with the assistance of the laser pump in 1964[1].

SBS is one of the strongest nonlinear optical effects. It has very useful application in many fields such as sensors,[2,3] narrow linewidth lasers,[4,5] slow and fast light,[6,7] light storage,[8] high resolution optical spectrometry[9,10] and microwave signal processing[11,12]. The harnessing of this effect includes the choice of proper materials for both light and acoustic waves and the optical enhancement structure. Optical fibers with the ability of confining light in a small mode area and a long distance have been successfully used to enhance and study the SBS processes. SBS has thus been demonstrated in traditional fibers,[2–12] photonics crystal fibers[13] and sub-wavelength microfibers[14]. On-chip optical waveguides are also very promising platforms for integrated solutions to harvest the SBS effect[15–17]. Based on these two waveguide structures, SBS on silica, silicon and chalcogenide with different gain profiles have been studied. However, to explore SBS effects in crystalline materials with low gain coefficient is challenging, which comes from the fact that the traditional fiber fabrication technique doesn't apply on crystals. Nevertheless, optical resonator structures such as whispering gallery mode (WGM) optical resonators can strongly enhance SBS in these materials and have become a solution.

A WGM resonator confines light through successive total internal reflections in an axisymmetric geometry. It can feature optical modes with very small mode volumes and ultrahigh quality (Q) factors. Such characteristics have made it a very suitable platform for investigating various nonlinear optical processes. Stimulated Raman, Brillouin scattering, third harmonic generation and four-wave

---

Nomenclature

FSR	free spectral range, GHz		λ	wavelength, m
n	refractive index		ν	resonance frequency, Hz
Q	quality factor		τ	resonance lifetime, s
v	acoustic wave speed, m/s			
			Subscripts	
Greek letters			a	acoustic
$\delta\nu$	resonance linewdith, Hz		B	Brillouin

mixing have been successfully demonstrated in WGM resonators made of fused silica in the past decade[18–22]. Potential applications of silica WGM resonator based SBS ranging from Brillouin cooling,[23] microwave synthesizer,[24] low-noise laser,[25] light storage,[26] slow and fast light[27] have been recently demonstrated. Crystalline WGM resonators with ultrahigh Q factors have been fabricated using precision mechanical polishing methods[28]. The material choices for such resonators include lithium niobate[28,29], barium borate[30,31], fluoride crystals[32–35], diamond[36] and so on. At this date, SBS has been reported in crystalline WGM resonators made of calcium fluoride[37] and barium fluoride[38]. Compared with other fluoride crystals, barium fluoride is an interesting scintillation crystal for high energy particle detection[39]. It also has a transparency further into the mid-infrared wavelength and an optimal anomalous dispersion profile[40]. The investigation of SBS in barium fluoride can thereby broaden potential applications in these fields.

In this article, we describe the development of WGM resonators based SBS technique. A rapidly scanning laser method is used to obtain the ringdown structure of the optical modes. The transmission spectrum shows a multimode structure of WGMs. We also show that the threshold power of SBS depends on the coupling gap between the resonator and the prism coupler. A 2.1 mW threshold power is reported in a centimeter scale barium fluoride resonator. Cascaded SBS with anti-Stokes is demonstrated.

2. Experimental setup

The WGM disk resonators used in this experiment were fabricated using a mechanical polishing method. The commercially available optical windows with diameter of 12 mm and thickness of 1 mm were used as raw preforms. The disk was first well centered and mounted on an air-bearing turning machine. Its rim where the optical WGM travels was then shaped into a "V" shape during the rough grinding process with large size abrasives (typically above 15 μm). The last step follows a fine optical polishing method with the size of diamond abrasives gradually down to sub-micrometer. The rim of the final disk has a sub-mm minor curvature and can feature a root mean square (rms) surface roughness in the range of few nanometers or even less[34]. Such an optically smooth surface is essentially required to support ultrahigh Q factor WGMs. Depending on the hardness of the material, the whole grinding and polishing procedure usually takes few hours. The major diameter of the final disk is slightly less than 12 mm. Crystalline resonators with Q factors above one billion have been fabricated from MgF_2, CaF_2 and BaF_2 crystals using this technique.

The experimental setup to study WGMs and stimulated Brillouin scattering is illustrated in Figure 1. The pump source is a Koheras continuous wave (CW) fiber laser at the wavelength of 1550 nm with the output power up to 200 mW. Its wavelength can be finely tuned through the high voltage piezo modulation input. A fiber polarization controller is used to optimize the coupling for different WGMs (TE or TM). The optical fiber circulator then extracts the feedback signal for detection through either a photodetector (PD2) or an ultrahigh resolution optical spectrum analyzer. Concerning the excitation of WGMs, the evanescent wave coupling method is adopted. We used an SF11 optical prism that has a higher refractive index for the coupling. The coupling part is put inside a clean chamber to avoid dust and air flow. The attenuated transmitted signal after the VOA is sent through a 3 dB fiber coupler.
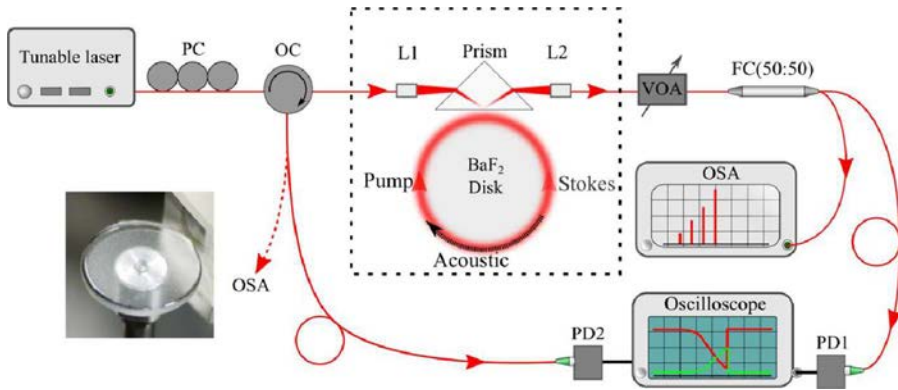
Figure 1. Experimental setup for the characterization of optical WGM resonators and the stimulated Brillouin scattering. PC: fiber polarization controller. OC: optical circulator. L1, L2: fiber lenses. VOA: variable optical attenuator. FC (50:50): 3 dB directional fiber coupler. OSA: optical spectrum analyzer. PD1, PD2: InGaAs photodetector. Inset: picture of the BaF$_2$ disk coupled by a SF11 prism.

The split signals are then analyzed with an ultrahigh resolution optical spectrum and a photodetector, respectively. The inset shows a photo of a BaF$_2$ disk coupled by an optical prism.

3. High quality factors

An interesting property of WGM optical resonators is their ability of tightly confining light for long periods of time. Such ability strongly enhances the light-matter interaction without the use of a long optical fiber. Because the photon lifetime is proportional to its Q factor, a sufficiently high Q factor becomes essential for studying various nonlinear optical effects with a low power pump laser operated in the CW regime. Q factors above one billion have been previously realized in various transparent crystalline materials such as quartz, sapphire, calcium fluoride, magnesium fluoride, barium fluoride and strontium fluoride[32–35]. The Q factor measurements include either linewidth measurement or ring down spectroscopy. The first method consists in obtaining the linewidth of a resonance $\delta\nu$, through $Q = \nu/\delta\nu$ where ν is the resonance frequency. It thus requires a probe laser with its linewidth smaller than that of the resonance. Moreover, as nonlinear effects or thermal effects can easily distort the shape of a WGM resonance, the probe laser power should also be kept as small as possible. To estimate the intrinsic Q factor, the coupling is usually operated in the far under-coupled regime, which is accomplished by increasing the evanescent wave coupling gap between the coupler and the resonator. In this condition, the measured loaded Q factor is very close to the intrinsic one. The other method measures the photon life time τ of a resonance since $Q = 2\pi\nu\tau$ through cavity ring down. In this way, the measurement will not be limited by the probe laser linewidth. In our experiment, we employ the second method to acquire the Q factor information of fluoride disks. Instead of using a fast shutter, a scanning ring down spectroscopy method is used here[41,42].

Figure 2(a) shows a typical transmission spectrum of a BaF$_2$ high-Q disk resonator coupled by an SF11 prism. The probe laser is swept across WGMs with a fast speed at 0.32 THz/s. Taking into account a free spectral range (FSR) of 5.5 GHz for this disk, the spanning range in Figure 2(a) actually covers about 30% of FSR. The multimode structure of WGMs is clearly visualized in this transmission spectrum. The resonant peaks correspond to different WGMs in the radial and polar directions similar to those in silica microspheres. In general, the polar order modes can be selectively excited by controlling the relative vertical coupling position of the disk[43]. One also notices that many resonance peaks have their transmission larger than unity, a result due to the ring down phenomenon. In these resonances, the light stored in the high Q resonator reemits and interfere with the probe laser[41]. A zoom in on a typical ring down spectrum is shown in Figure 1(b). A theoretical fit gives an intrinsic Q factor of 1.3×10^9.
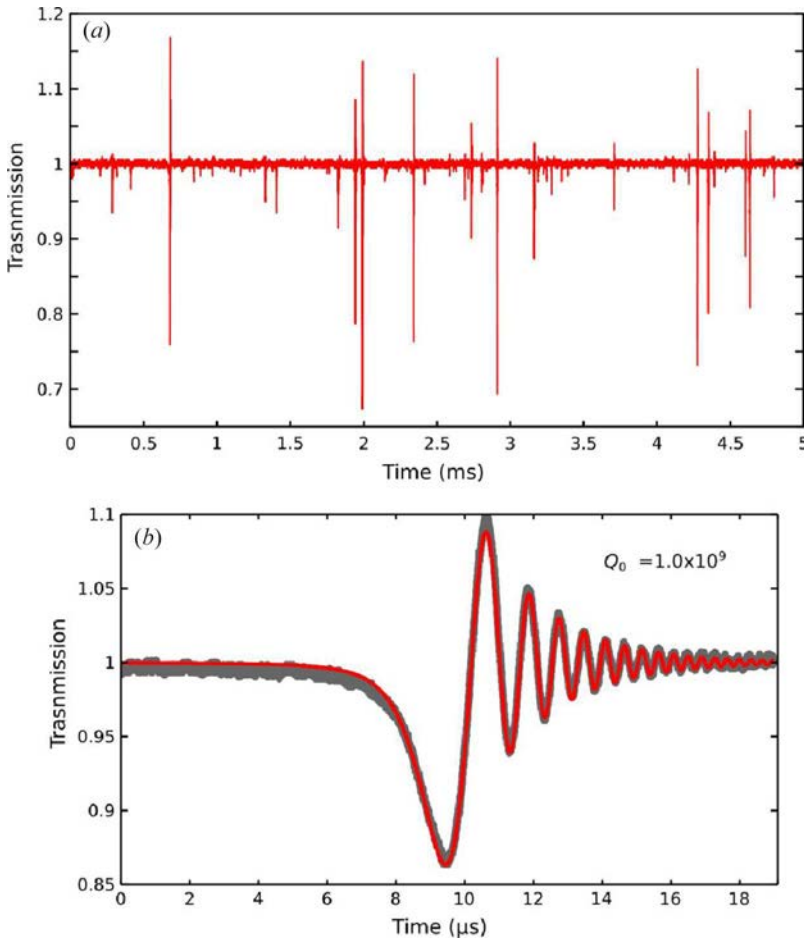
Figure 2. Transmission spectra of the resonator-prism coupling setup by PD1. (*a*) The pump laser is swept across WGM resonances over 1.6 GHz spectral range within 5 ms. (*b*) A zoom in of a WGM resonance featuring a ring down phenomenon due to ultrahigh Q factors. A theoretical fit gives an intrinsic linewidth of 1.0×10^9.

4. Stimulated Brillouin scattering and its threshold

The observation of ultrahigh Q factors is essential for reducing the SBS threshold power. However, the double-resonance condition should also be fulfilled to realize a lasing effect based on the SBS gain, similar to rare earth lasers. To now, most of Brillouin lasers are based on fiber ring resonators, as they can easily have a FSR that is smaller than the SBS gain bandwidth to ensure the double-resonance condition. It is known that the SBS effect has a typical bandwidth of tens of MHz and a frequency shift of the order of few GHz. For example, calcium fluoride crystal has a measured SBS gain bandwidth of 12 MHz[44]. Therefore, it is very challenging to realize a crystalline Brillouin laser based on a single mode fiber ring structure. Nevertheless, the multimode structure of WGMs as shown in Figure 2(*a*) can facilitate the realization of this condition. In a centimeter-scale WGM resonator, Brillouin lasing can be observed in several modes pumped by a mW level CW laser within one FSR[38].

Traditional threshold power measurements require a stable operation by locking the pump laser to the resonance wavelength. However, it has been demonstrated that the nonlinear thermal effect can enable a fast laser characterization and optimization technique in rare earth WGM microlasers[45]. We thus choose this technique for the Brillouin laser threshold power measurement. It should be mentioned that thermal effects in optical WGM resonators usually involve the thermo-optic effect, thermal expansion and Kerr effect. The thermal expansion of a centimeter-scale crystal is a relatively
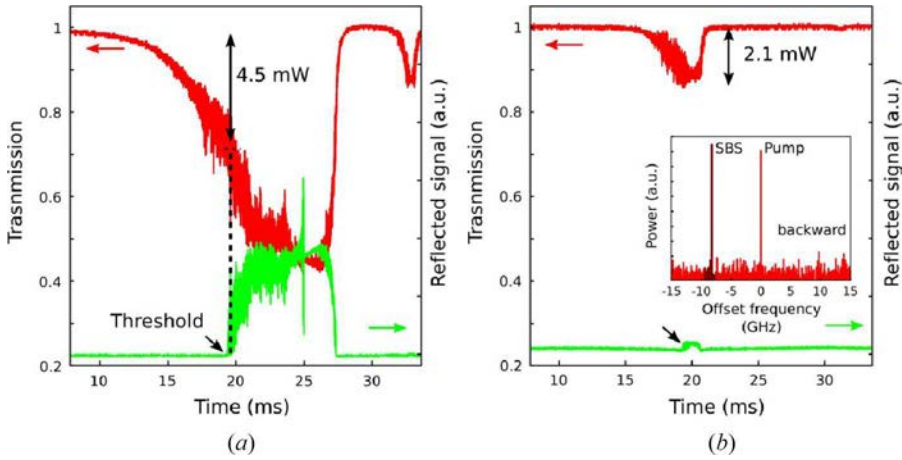
Figure 3. Simultaneous recording of the transmitted pump and the reflected signals. Upper curve: the transmission of the pump in PD1. Lower curve: the reflected signal in PD2. (a) The action of SBS is observed with an absorbed pump threshold of 4.5 mW. (b) An increased coupling gap reduces the coupling efficiency but decreases the absorbed pump threshold for SBS lasing. Inset: the corresponding optical spectrum in the backward direction.

slow process, as it needs time for the heat to dissipate into the whole resonator. On the other hand, the Kerr effect is a very fast process but it requires a high pump power. As a result, we believe that the thermal distortion of WGM resonances during the threshold power measurement is dominated by the thermo-optic effect of the material. Considering that BaF_2 crystal has a negative thermo-optic coefficient, it is thereby expected to have a broadened resonance on the wavelength-decreasing side of the laser ramping for a BaF_2 WGM disk as shown in Figure 3. The incident pump power at the input lens before the prism is 17.8 mW. As the pump laser wavelength is decreasing towards a WGM resonance, the coupled pump heats the crystal and causes a blue shift of the resonance, which is in the same direction of the laser scanning. The broadened resonance in turn assists the direct observation of the Brillouin laser.

In Figure 3, the transmitted pump signal (upper curve) and the backward Brillouin signal (lower curve) are simultaneously monitored. The arrow marks the action of the Brillouin lasing. The corresponding absorbed pump power is also highlighted. Figure 3(a, b) is obtained with different coupling gaps between the prism and the resonator, which is controlled by a piezo actuator. One notices that a larger gap puts the coupling into under-coupling regime but results in a smaller Brillouin threshold power (from 4.5 mW to 2.1 mW). It is mainly due to the increased loaded Q factor in this regime. However, it should also be noted that the change of the coupling condition could also affect the spatial and spectral overlaps of the pump mode and the Brillouin lasing mode. In general, the threshold performance is affected by the combination of these effects. The inset in Figure 3(b) shows the feedback optical spectrum when the coupled pump power is slightly above the threshold. A new frequency component with a frequency red shift of 8.2 GHz is observed. The frequency shift is in a good agreement with the Brillouin frequency shift in BaF_2. It is determined by the equation $\nu_B = 2n\nu_a/\lambda$ with n being the refractive index, ν_a the speed of acoustic wave and λ the wavelength of light wave, which is set by the phase matching condition of backward SBS. The pump signal in the backward direction could be due to the Rayleigh scattering in the resonator and some stray feedback in the coupling setup.

5. Cascaded stimulated Brillouin scattering

To further investigate the SBS phenomenon in BaF_2, we locked the pump laser frequency to a WGM resonance via the Pound-Drever-Hall (PDH) laser locking method[46] and increased the incident laser
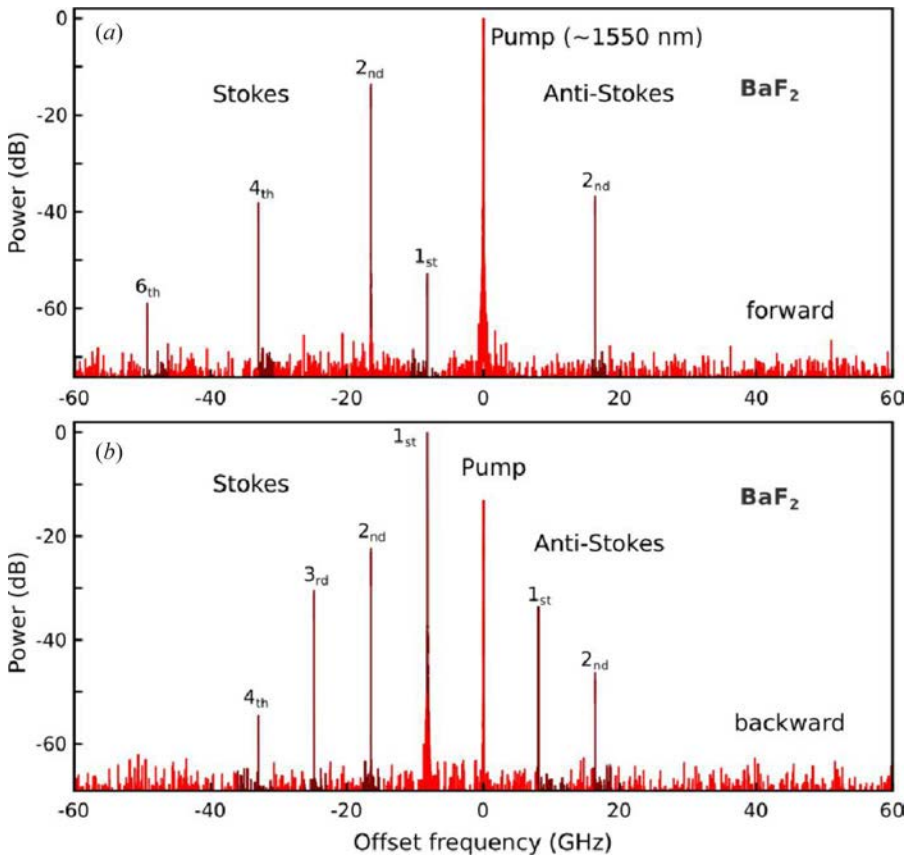
Figure 4. Cascaded Brillouin scattering in a BaF2 disk resonator pumped at 1550 nm. (*a*) In the forward direction. (*b*) In the backward direction. The observation of the anti-Stokes could be due to the four-wave mixing process, when considering the fact that the double SBS frequency shift could coincide with the triple FSR of the resonator.

power to around 80 mW. Figure 4(*a*, *b*) shows the optical spectra in the both forward and backward direction where multiple new frequency components occur. The ultrahigh Q factors and multi-resonance conditions fulfilled in such a centimeter scale resonator lead to the realization of Cascaded SBS. Single SBS can also be realized with selected pumping when these conditions are not fulfilled for the Second Stokes[38]. It is worth noting that the 5th Stokes component is missing in the backward direction as shown in Figure 4(*b*). Nevertheless, we still obtain the 6th Stokes in the corresponding forward direction in Figure 4(*a*). Considering the fact that the double SBS shift could happen to coincide the triple FSR of 16.5 GHz, we believe that the 6th Stokes is a result of the four-wave mixing (FWM) process. Therefore, the anti-Stokes components could also come from FWM between the pump and the Stokes or between the Stokes.

6. Conclusions

In conclusion, we have investigated the stimulated Brillouin scattering phenomenon in whispering gallery mode disk resonators. We observe multimode structures in a centimeter scale resonator made of BaF$_2$ crystal. The ring down spectroscopy with a rapidly scanning laser reveals that different ultrahigh Q modes can exist within one FSR of the resonator. We also study the SBS threshold performance by using the nonlinear cavity thermal effect. We show that SBS action starts with a mW level coupled pump power. The threshold also depends strongly on the coupling condition. The increased loaded Q factor in the undercoupled regime can lead to a decreased threshold. Futhermore, we haved realized

cascaded Brillouin scattering in such a resonator with up to the 6th Stokes (49 GHz frequency shift). Anti-Stokes components are also observed. This work shows that the WGM disk resonator platform can facilitate the investigation and harvesting of stimulated Brillouin scattering.

Funding

References

[1] Chiao, R.Y.; Townes, C.H.; Stoicheff, B.P. Stimulated Brillouin scattering and coherent generation of intense hypersonic waves. *Phys. Rev. Lett.* **1964**, *12*, 592–595.

[2] Foaleng, S.M.; Tur, M.; Beugnot, J.C.; Thevenaz, L. High spatial and spectral resolution long-range sensing using Brillouin echoes. *J. Lightwave Technol.* **2010**, *28*, 2993–3003.

[3] Chin, S.; Primerov, N.; Thevenaz, L. Sub-centimeter spatial resolution in distributed fiber sensing based on dynamic Brillouin grating in optical fibers. *IEEE Sens. J.* **2012**, *12*, 189–194.

[4] Smith, S.P.; Zarinetchi, F.; Ezekiel, S. Narrow-linewidth stimulated Brillouin fiber laser and applications. *Opt. Lett.* **1991**, *16*, 393–395.

[5] Ou, Z.; Bao, X.; Li, Y.; Saxena, B.; Chen, L. Ultranarrow linewidth Brillouin fiber laser. *IEEE Photonics Technol. Lett.* **2014**, *26*, 2058–2061.

[6] Gonzalez-Herraez, M.; Song, K.Y.; Thevenaz, L. Optically controlled slow and fast light in optical fibers using stimulated Brillouin scattering. *Appl. Phys. Lett.* **2005**, *87*, 081113.

[7] Okawachi, Y.; Bigelow, M.S.; Sharping, J.E.; Zhu, Z.M.; Schweinsberg, A.; Gauthier, D.J.; Boyd, R.W.; Gaeta, A.L. Tunable all-optical delays via Brillouin slow light in an optical fiber. *Phys. Rev. Lett.* **2005**, *94*, 153902.

[8] Zhu, Z.; Gauthier, D.J.; Boyd, R.W. Stored light in an optical fiber via stimulated Brillouin scattering. *Science.* **2007**, *318*, 1748–1750.

[9] Subias Domingo, J.M.; Pelayo, J.; Villuendas, F.; Heras, C.D.; Pellejer, E. Very high resolution optical spectrometry by stimulated Brillouin scattering. *IEEE Photonics Technol. Lett.* **2005**, *17*, 855–857.

[10] Schneider, T. Wavelength and line width measurement of optical sources with femtometre resolution. *Electron. Lett.* **2005**, *41*, 1234–1235.

[11] Vidal, B.; Piqueras, M.A.; Marti, J. Tunable and reconfigurable photonic microwave filter based on stimulated Brillouin scattering. *Opt. Lett.* **2007**, *32*, 23–25.

[12] Chin, S.; Thevenaz, L.; Sancho, J.; Sales, S.; Capmany, J.; Berger, P.; Bourderionnet, J.; Dolfi, D. Broadband true time delay for microwave signal processing, using slow light based on stimulated Brillouin scattering in optical fibers. *Opt. Express* **2010**, *18*, 22599–22613.

[13] Dainese, P.; Russell, P.S.J.; Joly, N.; Knight, J.C.; Wiederhecker, G.S.; Fragnito, H.L.; Laude, V; Khelif, A. Stimulated Brillouin scattering from multi-GHz-guided acoustic phonons in nanostructured photonic crystal fibres. *Nature Phys.* **2006**, *2*, 388–392.

[14] Beugnot, J.-C.; Lebrun, S.; Pauliat, G.; Maillotte, H.; Laude V.; Sylvestre, T. Brillouin light scattering from surface acoustic waves in a subwavelength-diameter optical fibre. *Nature Commun.* **2014**, *5*, 5242.

[15] Pant, R.; Poulton, C.G.; Choi, D.Y.; McFarlane, H.; Hile, S.; Li, E.; Thevenaz, L.; Luther-Davies, B.; Madden, S.J.; Eggleton, B.J. On-chip stimulated Brillouin scattering. *Opt. Express* **2011**, *19*, 8285–8290.

[16] Rakich, P.T.; Reinke, C.; Camacho, R.; Davids, P.; Wang, Z. Giant enhancement of stimulated Brillouin scattering in the subwavelength limit. *Phys. Rev. X* **2012**, *2*, 011008.

[17] Shin, H.; Qiu, W.; Jarecki, R.; Cox, J.A.; Olsson, R.H.; Starbuck, A.; Wang, Z.; Rakich, P.T. Tailorable stimulated Brillouin scattering in nanoscale silicon waveguides. *Nat. Commun.* **2013**, *4*, 1944.

[18] Spillane, S.M.; Kippenberg, T.J.; Vahala, K.J. Ultralow-threshold Raman laser using a spherical dielectric microcavity. *Nature* **2002**, *415*, 621–623.

[19] Tomes, M.; Carmon, T. Photonic micro-electromechanical systems vibrating at X-band (11-GHz) rates. *Phys. Rev. Lett.* **2009**, *102*, 113601.

[20] Carmon, T.; Vahala, K.J. Visible continuous emission from a silica microphotonic device by third-harmonic generation. *Nature Phys.* **2007**, *3*, 430–435.

[21] Kippenberg, T.J.; Spillane, S.M.; Vahala, K.J. Kerr-nonlinearity optical parametric oscillation in an ultrahigh-Q toroid microcavity. *Phys. Rev. Lett.* **2004**, *93*, 083904.

[22] Del'Haye, P.; Schliesser, A.; Arcizet, O.; Wilken, T.; Holzwarth, R.; Kippenberg, T.J. Optical frequency comb generation from a monolithic microresonator. *Nature* **2007**, *450*, 1214–1217.

[23] Bahl, G.; Tomes, M.; Marquardt, F.; Carmon, T. Observation of spontaneous Brillouin cooling. *Nat. Phys.* **2012**, *8*, 203–207.

[24] Li, J.; Lee, H.; Vahala, K.J. Microwave synthesizer using an on-chip Brillouin oscillator. *Nat. Commun.* **2013**, *4*, 2097.

[25] Li, J.; Lee, H.; Vahala, K.J. Low-noise Brillouin laser on a chip at 1064 nm. *Opt. Lett.* **2014**, *39*, 287–290.

[26] Dong, C.H.; Shen, Z.; Zou C.L.; Zhang Y.L.; Fu W.; Guo, G.C. Brillouin-scattering-induced transparency and non-reciprocal light storage. *Nat. Commun.* **2015**, *6*, 6193.

[27] Kim, J.; Kuzyk, M.C.; Han, K.; Wang, H.; Bahl, G. Non-reciprocal Brillouin scattering induced transparency. *Nat. Phys.* **2015**, *11*, 275–280.

[28] Ilchenko, V.S.; Savchenkov, A.A.; Matsko, A.B.; Maleki, L. Nonlinear optics and crystalline whispering gallery mode cavities. *Phys. Rev. Lett.* **2004**, *92*, 043903.

[29] Fürst, J.U.; Strekalov, D.V.; Elser, D.; Lassen, M.; Andersen, U.L.; Marquardt, C.; Leuchs, G. Naturally phase-matched second-harmonic generation in a whispering-gallery-mode resonator. *Phys. Rev. Lett.* **2010**, *104*, 153901.

[30] Lin, G.; Fürst, J.; Strekalov, D.V.; Grudinin, I.S.; Yu, N. High-Q UV whispering gallery mode resonators made of angle-cut BBO crystals. *Opt. Express* **2012**, *20*, 21372–21378.

[31] Lin, G.; Fürst, J.U.; Strekalov, D.V.; Yu, N. Wide-range cyclic phase matching and second harmonic generation in whispering gallery resonators. *Appl. Phys. Lett.* **2013**, *103*, 181107.

[32] Savchenkov, A.A.; Ilchenko, V.S.; Matsko, A.B.; Maleki, L. Kilohertz optical resonances in dielectric crystal cavities. *Phys. Rev. A* **2004**, *70*, 051804.

[33] Liang, W.; Savchenkov, A.A.; Matsko, A.B.; Ilchenko, V.S.; Seidel, D.; Maleki, L. Generation of near-infrared frequency combs from a MgF 2 whispering gallery mode resonator. *Opt. Lett.* **2011**, *36*, 2290–2292.

[34] Lin, G.; Diallo, S.; Henriet, R.; Jacquot, M.; Chembo, Y.K. Barium fluoride whispering-gallery-mode disk-resonator with one billion quality-factor. *Opt. Lett.* **2014**, *39*, 6009–6012.

[35] Henriet, R.; Lin, G.; Coillet, A.; Jacquot, M.; Furfaro, L.; Larger, L.; Chembo, Y.K. Kerr optical frequency comb generation in strontium fluoride whispering-gallery mode resonators with billion quality factor. *Opt. Lett.* **2015**, *40*, 1567–1570.

[36] Ilchenko, V.S.; Bennett, A.M.; Santini, P.; Savchenkov, A.A.; Matsko, A.B.; Maleki, L. Whispering gallery mode diamond resonator. *Opt. Lett.* **2013**, *38*, 4320–4323.

[37] Grudinin, I.S.; Matsko, A.B.; Maleki, L. Brillouin lasing with a CaF 2 whispering gallery mode resonator. *Phys. Rev. Lett.* **2009**, *102*, 043902.

[38] Lin, G.; Diallo, S.; Saleh, K.; Martinenghi, R.; Beugnot, J.C.; Sylvestre, T.; Chembo, Y.K. Cascaded Brillouin lasing in monolithic barium fluoride whispering gallery mode resonators. *Appl. Phys. Lett.* **2014**, *105*, 231103.

[39] Han, H.; Zhang, Z.; Weng, X.; Liu, J.; Guan, X.; Zhang, K.; Li, G. Development of a fast radiation detector based on barium fluoride scintillation crystal. *Rev. Sci. Instrum.* **2013**, *84*, 073503.

[40] Lin, G.; Chembo, Y.K. On the dispersion management of fluorite whispering-gallery mode resonators for Kerr optical frequency comb generation in the telecom and mid-infrared range. *Opt. Express* **2015**, *23*, 1594–1604.

[41] Savchenkov, A.A.; Matsko, A.B.; Ilchenko, V.S.; Maleki, L. Optical resonators with ten million finesse. *Opt. Express* **2007**, *15*, 6768–6773.

[42] Dumeige, Y.; Trebaol, S.; Ghişa, L.; Nguyen, T.K.N.; Tavernier, H.; Féron, P. Determination of coupling regime of high-Q resonators and optical gain of highly selective amplifiers. *J. Opt. Soc. Am. B* **2008**, *25*, 2073–2080.

[43] Lin, G.; Qian, B.; Oručević, F.; Candela, Y.; Jager, J.B.; Cai, Z.; Lefèvre-Seguin, V.; Hare, J. Excitation mapping of whispering gallery modes in silica microcavities. *Opt. Lett.* **2010**, *35*, 583–585.

[44] Sonehara, T.; Konno, Y.; Kaminaga, H.; Saikan, S.; Ohno, S. Frequency-modulated stimulated Brillouin spectroscopy in crystals. *J. Opt. Soc. Am. B* **2007**, *24*, 1193–1198.

[45] Lin, G.; Candela, Y.; Tillement, O.; Cai, Z.; Lefèvre-Seguin, V.; Hare, J. Thermal bistability-based method for real-time optimization of ultralow-threshold whispering gallery mode microlasers. *Opt. Lett.* **2012**, *37*, 5193–5195.

[46] Drever, R.W.P.; Hall, J.L.; Kowalski, F.V.; Hough, J.; Ford, G.M.; Munley, A.J.; Ward, H. Laser phase and frequency stabilization using an optical resonator. *Appl. Phys. B* **1983**, *31*, 97–105.